Bosonic Analogue of Dirac Composite Fermi Liquid

David F. Mross,[1] Jason Alicea,[1,2] and Olexei I. Motrunich[1,2]
[1]Department of Physics and Institute for Quantum Information and Matter, California Institute of Technology, Pasadena, California 91125, USA
[2]Walter Burke Institute for Theoretical Physics, California Institute of Technology, Pasadena, California 91125, USA
(Received 24 May 2016; published 22 September 2016)

We introduce a particle-hole-symmetric metallic state of bosons in a magnetic field at odd-integer filling. This state hosts composite fermions whose energy dispersion features a quadratic band touching and corresponding 2π Berry flux protected by particle-hole and discrete rotation symmetries. We also construct an alternative particle-hole symmetric state—distinct in the presence of inversion symmetry—without Berry flux. As in the Dirac composite Fermi liquid introduced by Son [Phys. Rev. X **5**, 031027 (2015)], breaking particle-hole symmetry recovers the familiar Chern-Simons theory. We discuss realizations of this phase both in 2D and on bosonic topological insulator surfaces, as well as signatures in experiments and simulations.

DOI: 10.1103/PhysRevLett.117.136802

Introduction.—The past year has seen numerous exciting developments in our understanding of electronic quantum-Hall states that resolved long-standing puzzles regarding particle-hole (PH) symmetry. At filling factor $\nu = 1/2$, electrons fill exactly half of the available single-particle orbitals in the lowest Landau level (LLL). Within that subspace, the system enjoys PH symmetry that is conspicuously absent in the classic Halperin-Lee-Read (HLR) theory [1–7]. There, *composite fermions*, obtained by attaching two flux quanta to electrons that cancel the applied field on average, fill a parabolic band and form a Fermi surface—i.e., a composite Fermi liquid (CFL). The corresponding Lagrangian density reads

$$\mathcal{L}_{\mathrm{CS}} = f^{\dagger}\left(i(D_0 - iA_0) - \frac{(\vec{D} - i\vec{A})^2}{2m^*}\right)f - \frac{k}{8\pi}\epsilon_{\kappa\mu\nu}a_\kappa\partial_\mu a_\nu, \tag{1}$$

where f is the composite-fermion field, A_μ (with $\mu = 0, 1, 2$) is the electromagnetic vector potential, $D_\mu = \nabla_\mu - ia_\mu$ denotes the covariant derivative with a_μ an emergent gauge field, and $k = 1$ is the level of the Chern-Simons (CS) term that attaches flux. Despite the absence of PH symmetry, the HLR theory is remarkably successful in predicting experimental results at and around $\nu = 1/2$.

To incorporate PH symmetry, Son proposed that composite fermions are Dirac particles at finite density coupled to an emergent gauge field [8] without a CS term:

$$\mathcal{L}_{\mathrm{QED}_3} = i\bar{\Psi}D_\mu\gamma^\mu\Psi - \frac{k}{4\pi}\epsilon_{\kappa\mu\nu}A_\kappa\partial_\mu a_\nu. \tag{2}$$

Here Ψ and $\bar{\Psi} = \Psi^\dagger\gamma^0$ are two-component spinors, while γ^μ are Dirac matrices. Equation (2) implements two important features of the half filled Landau level: (i) The Dirac composite fermions are neutral under A_μ [9–12] and (ii) the theory preserves the antiunitary PH transformation

$$\mathcal{C}\Psi\mathcal{C}^{-1} = i\sigma^2\Psi, \qquad \mathcal{C}(a_0, \vec{a})\mathcal{C}^{-1} = (a_0, -\vec{a}). \tag{3}$$

References [13–20] support Son's theory and the presence of PH symmetry at $\nu = 1/2$.

These developments prompt us to revisit the CFL formed by bosons at $\nu = 1$, where flux attachment yields Eq. (1) with $k = 2$. Importantly, bosonic integer-quantum-Hall (IQH) states do not admit a single-particle description, which obscures a precise definition of PH symmetry even when restricting to the LLL. To access PH-symmetric CFLs of $\nu = 1$ bosons, we therefore follow a two-pronged approach: First, we study bosons at a "plateau transition" [21] between a $\nu = 2$ IQH state [22–24] and the vacuum [25,26]. Upon fine-tuning, the critical theory exhibits a PH symmetry analogous to the electronic case, in addition to microscopic inversion symmetry. Second, we consider the surface of a particular 3D symmetry protected topological phase (SPT) of bosons [27], where both symmetries can be realized microscopically.

These methods suggest a natural bosonic analogue of Eq. (2) given by

$$\mathcal{L}_{\mathrm{CFL}_{2\pi}} = \Psi^\dagger\begin{pmatrix} iD_0 & (D_1 + iD_2)^2 \\ (D_1 - iD_2)^2 & iD_0 \end{pmatrix}\Psi - \frac{1}{2\pi}\epsilon_{\kappa\mu\nu}A_\kappa\partial_\mu a_\nu. \tag{4}$$

Note that the composite-fermion density is dynamically fixed to $n_{\mathrm{CF}} = (\partial_1 A_2 - \partial_2 A_1)/2\pi$. The first line of Eq. (4) also describes electronic excitations of bilayer graphene [28]. In the present context, composite fermions analogously exhibit a single quadratic band touching that is protected against weak perturbations that respect both PH symmetry $\mathcal{C}$ and fourfold rotation symmetry $\mathcal{R}(\pi/2)$ (see Fig. 1). With inversion symmetry $\mathcal{I}$ instead of $\mathcal{R}(\pi/2)$, the spectrum generically splits into two massless Dirac cones, similar to the effect of trigonal warping in bilayer graphene [28]. At suitable doping, either case features a single Fermi surface enclosing 2π Berry flux.

To distinguish different kinds of PH-symmetric CFLs, we adopt notation $\mathrm{CFL}_{k\pi}$, where $k\pi$ is the Berry flux enclosed in

 © 2016 American Physical Society

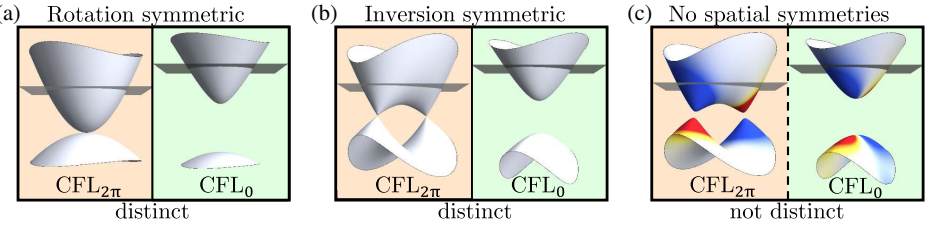

FIG. 1. Composite-fermion band structures for $\mathrm{CFL}_{2\pi}$ and CFL_0 states with PH symmetry and varying spatial symmetries. Horizontal planes indicate the chemical potentials of interest. (a) With fourfold rotation symmetry, $\mathrm{CFL}_{2\pi}$ exhibits a protected quadratic band touching, unlike CFL_0. (b) Breaking rotation down to inversion symmetry allows the band touching to split into two protected Dirac cones but preserves the 2π Berry flux. (c) Lifting inversion symmetry generically splits the bands, resulting in nonzero Berry curvature indicated by color (blue and red for opposite signs). The sharp distinction between $\mathrm{CFL}_{2\pi}$ and CFL_0 then disappears. Away from degeneracy points, PH and inversion symmetries, respectively, constrain the Berry curvature $\mathcal{B}$ at momentum $\mathbf{k}$ as $\mathcal{B}(\mathbf{k}) = -\mathcal{B}(-\mathbf{k})$ and $\mathcal{B}(\mathbf{k}) = \mathcal{B}(-\mathbf{k})$; the presence of both symmetries [i.e., cases (a) and (b)] thus implies $\mathcal{B} = 0$.

the composite-fermion Fermi surface. Thus, the fermionic $\nu = 1/2$ state described by $\mathcal{L}_{\mathrm{QED}_3}$ corresponds to CFL_π, while the bosonic state described by $\mathcal{L}_{\mathrm{CFL}_{2\pi}}$ is $\mathrm{CFL}_{2\pi}$. As we will see, an alternative $\mathcal{C}$- and $\mathcal{I}$-symmetric state for bosons, CFL_0, with zero Berry flux is also possible. For any $\mathrm{CFL}_{k\pi}$, weak PH symmetry breaking splits the bands, and subsequently integrating out the negative energy states generates a level-k CS term as in $\mathcal{L}_{\mathrm{CS}}$ (i.e., no CS term for $k = 0$). Absent inversion symmetry, the sharp distinction between $\mathrm{CFL}_{2\pi}$ and CFL_0 disappears.

Bosons at $\nu = 1$ as a plateau transition.—Consider a system composed of narrow strips of width d along the y direction and infinite along x; see Fig. 2(a). The boson density ρ for adjacent strips alternates between ρ_0 and 0, and a uniform perpendicular magnetic field $B = (ch\rho_0)/2e$ yields filling factor $\nu = (ch\rho)/eB = 2$ for the ρ_0 strips. At length scales much larger than d, we thus obtain bosons with average filling $\nu = 1$.

We require each $\nu = 2$ strip to form a bosonic IQH state [22–24,29] that hosts edge states with two flavors $\alpha = \pm$ of charge-e bosons. Labeling the edges by integers y (cf. Fig. 2) and corresponding bosons by $b_{y,\alpha} \sim e^{i\phi_{y,\alpha}}$, the Lagrangian density for the lower (odd y) and upper (even y) edges is

$$\mathcal{L}_{\mathrm{edge}} = \frac{(-1)^y K_{\alpha\alpha'}}{4\pi}\partial_x\phi_{y,\alpha}\partial_t\phi_{y,\alpha'} + \frac{u}{4\pi}(\partial_x\phi_{y,\alpha})^2, \quad (5)$$

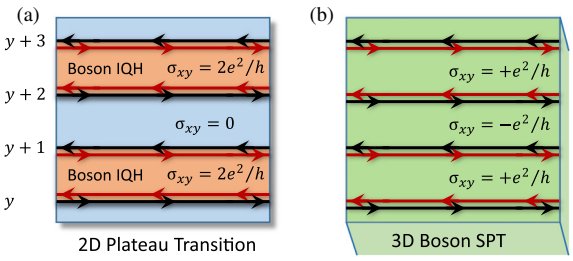

FIG. 2. (a) Alternating strips of bosons at $\nu = 2$ and $\nu = 0$ yield an average filling $\nu = 1$. Edges contain a chiral charge mode and a counterpropagating neutral mode, described by the K matrix σ^x. (b) The same edge-state network arises on the surface of a 3D bosonic SPT with $U(1) \times \mathcal{C}$ symmetry when the antiunitary PH symmetry $\mathcal{C}$ is broken oppositely for neighboring strips.

where $K = \sigma^x$. Here and below α and α' are implicitly summed.

To access 2D CFLs, we allow tunneling between neighboring edges. For example, flavor-conserving tunnelings read

$$\mathcal{L}_{\mathrm{hop}} = w_{y,\alpha}(e^{i(2\pi eB/hc)dx}b^\dagger_{y+1,\alpha}b_{y,\alpha} + \mathrm{c.c.}); \quad (6)$$

i.e., the edge bosons $b_{y,\alpha}$ experience a uniform magnetic field. Our setup preserves a microscopic inversion symmetry [29],

$$\mathcal{I}b_{y,\alpha}(x)\mathcal{I}^{-1} = b_{1-y,-\alpha}(-x) \quad (\text{inversion}), \quad (7)$$

that constrains the hopping amplitudes via $w_{y,\alpha} = w_{-y,-\alpha}$. With translation invariance $y \to y + 2$, only $w_{y=\mathrm{even}}$ (hopping across vacuum) and $w_{y=\mathrm{odd}}$ (hopping across IQH strips) are independent. When they are fine-tuned to be equal, the low-energy theory $\mathcal{L}_{\mathrm{hop}} + \mathcal{L}_{\mathrm{edge}}$ additionally exhibits an emergent antiunitary PH symmetry:

$$\mathcal{C}b_{y,\alpha}\mathcal{C}^{-1} = b^\dagger_{y+1,\alpha} \quad (\text{particle hole}). \quad (8)$$

This symmetry has the desired properties that it squares to unity and relates bosons at ν to bosons at $2 - \nu$ [31].

3D boson SPT surface.—Closely related physics can appear at the surface of a 3D bosonic SPT [32] with a conserved charge that is odd under a local antiunitary PH symmetry, i.e., $U(1) \times \mathcal{C}_{\mathrm{local}}$ [31,33]. This symmetry pins the chemical potential to zero but permits an orbital magnetic field. Breaking $\mathcal{C}_{\mathrm{local}}$ generates a gapped, unfractionalized surface with Hall conductance $\sigma_{xy} = \pm e^2/h$. At boundaries between domains with oppositely broken $\mathcal{C}_{\mathrm{local}}$, the Hall conductance changes by $2e^2/h$—implying gapless edge states described by Eq. (5). A surface that hosts alternating $\pm e^2/h$ strips of equal width [Fig. 2(b)] breaks $\mathcal{C}_{\mathrm{local}}$ but retains this symmetry when composed with a translation T_y by one strip width, i.e., Eq. (8) with $\mathcal{C} = \mathcal{C}_{\mathrm{local}}T_y$. Note that unlike the 2D plateau transition, $\mathcal{C}$ is a microscopic symmetry on the SPT surface.

Bosonic CFLs.—Both the plateau-transition and SPT-surface realization lead us to study $\mathcal{L}_{\mathrm{edge}} + \mathcal{L}_{\mathrm{hop}}$. Our analysis is facilitated by explicit duality mappings for such

network models [18] that relate SPT surfaces to quantum electrodynamics in $(2+1)$ dimensions (QED_3) described by $\mathcal{L}_{QED_3}$. (See also Refs. [13,34] and Refs. [25,26,35–37] for the fermionic and bosonic cases, respectively, and Refs. [38–40] for recent developments.) The dual composite-fermion density is proportional to the physical magnetic field B, while the number of flavors N_f depends on the statistics of the microscopic particles forming the SPT:

$$\text{3D electron SPT surface} \leftrightarrow N_f = 1 \text{ QED}_3,$$

$$\text{3D boson SPT surface} \leftrightarrow N_f = 2 \text{ QED}_3.$$

Either bosonic setup from Fig. 2 thus maps to $\mathcal{L}_{QED_3}$ in Eq. (2) with $k=2$ and $N_f=2$.

We will package the two flavors into a single four-component spinor Ψ_4 and use Dirac matrices $\gamma^0=\tau^0\sigma^z$, $\gamma^1=i\tau^0\sigma^y$, $\gamma^2=-i\tau^0\sigma^x$, where σ^μ and τ^μ are, respectively, intra- and interflavor Pauli matrices. Following the mapping from Ref. [18], the symmetries in Eqs. (7) and (8) act as [41]

$$\mathcal{C}\Psi_4\mathcal{C}^{-1}=\sigma^y\tau^y\Psi_4, \qquad \mathcal{I}\Psi_4\mathcal{I}^{-1}=\sigma^z\tau^z\Psi_4. \tag{9}$$

The continuum dual QED_3 theory also preserves continuous rotations

$$\mathcal{R}(\Phi)\Psi_4(\vec{x})\mathcal{R}^{-1}(\Phi)=e^{i(\Phi/2)(\tau^z+\sigma^z)}\Psi_4[\mathcal{R}(\Phi)\vec{x}] \tag{10}$$

with $\mathcal{R}(\pi)=\mathcal{I}$. While $\mathcal{R}$ is not a microscopic symmetry of the network model, we expect it to be relevant for CFL realizations in isotropic systems.

We thus first analyze a composite-fermion Hamiltonian $H_\mathcal{R}=\Psi_4^\dagger h_\mathcal{R}\Psi_4$ containing general momentum-independent bilinears preserving both $\mathcal{C}$ and $\mathcal{R}(\pi/2)$ [42]:

$$h_\mathcal{R}=i\sigma^xD_1+i\sigma^yD_2-\Delta\tau^z\sigma^z+g(\tau^x\sigma^x+\tau^y\sigma^y). \tag{11}$$

At mean-field level (neglecting a_μ) the spectrum contains four bands, labeled as positive and negative according to their large-k asymptotics, i.e.,

$$E_{\text{positive}}(\vec{k})=\pm g+\sqrt{\vec{k}^2+(g\pm\Delta)^2}, \tag{12}$$

$$E_{\text{negative}}(\vec{k})=\pm g-\sqrt{\vec{k}^2+(g\pm\Delta)^2}. \tag{13}$$

Several distinct regimes are accessible depending on g and Δ, as sketched in Figs. 3(a)–3(d): (a) For $g=\Delta=0$, we recover two massless Dirac cones. (b) At finite $|g|>|\Delta|$, a quadratic band touching emerges; the $CFL_{2\pi}$ state then appears when the chemical potential intersects only one of the central bands as in Fig. 3(b). In this case, one can project onto states close to the band touching (see Supplemental Material [29]), yielding Eq. (4) with two-component spinors Ψ_2 that transform as

$$\mathcal{C}\Psi_2\mathcal{C}^{-1}=\sigma^x\Psi_2, \quad \mathcal{R}(\Phi)\Psi_2\mathcal{R}^{-1}(\Phi)=e^{i\Phi\sigma^z}\Psi_2. \tag{14}$$

The only perturbation allowed by $\mathcal{R}(\pi/2)$ up to $\mathcal{O}(k^2)$ is the $\mathcal{C}$-odd mass term $\Psi_2^\dagger\sigma^z\Psi_2$. Thus, $CFL_{2\pi}$ with quadratic band touching is stable with these symmetries. Relaxing

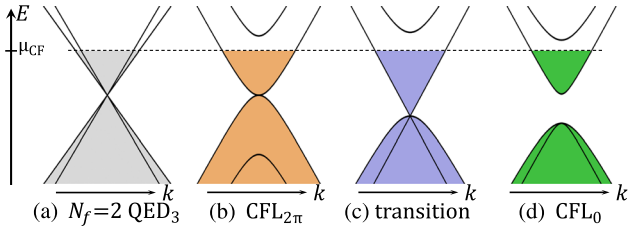

FIG. 3. (a) Massless Dirac band structure for "pure" $N_f=2$ QED_3 that is dual to the bosonic models studied here (shown with different velocities to emphasize $N_f=2$). The magnetic field for the bosons maps to a nonzero composite-fermion density that yields two Fermi surfaces. (b) PH and rotation-symmetric perturbations with $|g|>|\Delta|$ yield $CFL_{2\pi}$ with a quadratic band touching and a single Fermi surface. (c) The transition between $CFL_{2\pi}$ and CFL_0 occurs at $|g|=|\Delta|$ where three bands meet at $k=0$. (d) For $|g|<|\Delta|$, one obtains CFL_0 featuring separated upper and lower bands and a single Fermi surface at an appropriate density. Note that the nature of the partially filled positive-energy band changes qualitatively, with the Berry flux jumping from 2π to 0.

$\mathcal{R}(\pi/2)\to\mathcal{I}$ allows the terms $\Psi_2^\dagger\sigma^{x,y}\Psi_2$, which split the band touching into two Dirac cones without opening a gap [see Fig. 1(b)]. Upon breaking inversion, the PH-symmetric terms $\Psi_2^\dagger\sigma^z i\partial_{1,2}\Psi_2$ gap out the two Dirac cones [Fig. 1(c)]. (c) At $|g|=|\Delta|$, the spectrum hosts a threefold band touching. (d) For $|g|<|\Delta|$, a gap opens and the conduction band "detaches" from the valence bands (see Supplemental Material [29] for details). The special point (c) thus marks the transition at which the topological winding associated with the quadratic band touching transfers to the bottom-most bands (for $\Delta>0$; with $\Delta<0$, the band order reverses). Integrating out these filled negative-energy bands does not generate a CS term. At suitable doping, one thus obtains a single Fermi surface with neither a CS term nor Berry curvature, corresponding to CFL_0.

We emphasize that the distinction between $CFL_{2\pi}$ and CFL_0 requires *both* PH and inversion symmetries, since breaking either generically splits the bands. When PH is

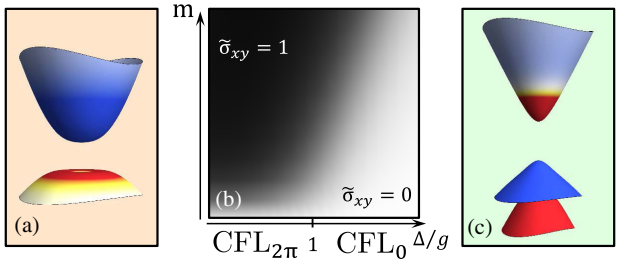

FIG. 4. Both $CFL_{2\pi}$ and CFL_0 exhibit vanishing composite-fermion Hall conductance $\tilde{\sigma}_{xy}=0$ due to PH symmetry $\mathcal{C}$. Upon breaking $\mathcal{C}$ by the term $m\Psi_2^\dagger\sigma^z\Psi_2$, $\tilde{\sigma}_{xy}=0$ crosses over to the HLR value $\tilde{\sigma}_{xy}=1$ (center). For $\Delta/g<1$, the $CFL_{2\pi}$ band touching is lifted by g, resulting in bands with opposite Berry curvature (left). For $\Delta/g>1$, the partially filled CFL_0 band develops Berry curvature as a function of m and changes sign between small and large momenta (right).

broken, generic Fermi surfaces enclose a nonuniversal nonquantized Berry flux (Fig. 4). On the other hand, breaking inversion symmetry while preserving PH always yields zero enclosed Berry flux [Fig. 1(c)].

Properties.—A useful device for determining the presence of PH symmetry in numerical studies is via $2K_F$ oscillations in the composite-fermion density $\tilde{\rho}$. In the electronic case, $\tilde{\rho}_{k\approx 2K_F}$ is PH odd and thus generically contributes to the physical charge density [15]. In the bosonic $\mathrm{CFL}_{2\pi}$ and CFL_0, by contrast, $\tilde{\rho}_{k\approx 2K_F}$ is PH even and does not contribute to the boson density ρ. Any $2K_F$ oscillations in the boson density thus directly probe PH-symmetry breaking.

One may be tempted to argue that a Berry phase $\gamma_{\mathrm{Berry}} = 2\pi$ is not meaningfully distinct from $\gamma_{\mathrm{Berry}} = 0$. Indeed, in a rotationally symmetric system the Berry phase may be computed as

$$\gamma_{\mathrm{Berry}} = -i \int_0^{2\pi} d\theta \langle u | \partial_\theta | u \rangle, \tag{15}$$

and a simple gauge transformation $|u\rangle \to e^{in\theta}|u\rangle$ changes γ_{Berry} by $2\pi n$. This ambiguity does not arise for nondegenerate bands which always feature a well-defined (smooth) local Berry curvature which can be integrated to a unique value for $\gamma_{\mathrm{Berry}} \in \mathbb{R}$. Here, the gauge transformation described above is singular at the origin and is thus not meaningful. A useful, physical way to resolve this issue is to lift the degeneracy by infinitesimally breaking particle-hole symmetry while retaining inversion symmetry. This results in $\pm 2\pi$ Berry flux in the partially filled positive-energy band in the $\mathrm{CFL}_{2\pi}$ regime and zero in the CFL_0 regime; cf. Eq. (16).

It is instructive to analyze how both $\mathrm{CFL}_{2\pi}$ and CFL_0 reduce to the conventional HLR state upon breaking PH symmetry. A useful quantity in this context is the composite-fermion Hall conductance $\tilde{\sigma}_{xy} = (k/2) - (\gamma/2\pi)$, where $k \in \mathbb{Z}$ is the level of the CS term for the emergent gauge field and $\gamma \in \mathbb{R}$ is the Berry flux enclosed in the Fermi surface that yields an anomalous Hall effect [8]. In the bosonic HLR state [Eq. (1)], $k = 2$ and $\gamma = 0$ so that $\tilde{\sigma}_{xy} = 1$. PH symmetry, however, demands $\tilde{\sigma}_{xy} = 0$ in both $\mathrm{CFL}_{2\pi}$ and CFL_0. For the former, breaking PH symmetry via $m\Psi_2^\dagger \sigma^z \Psi_2$ splits the bands [Fig. 4(a)], whereupon integrating out the negative-energy states generates a $k = 2$ CS term. In contrast, weakly breaking PH symmetry in CFL_0 does not produce a CS term but induces a nonzero Berry curvature in the partially filled band; see Fig. 4(c) and Supplemental Material [29] for details. The two cases can be summarized as

$$\begin{aligned} k_{\mathrm{CFL}_{2\pi}} &= 2, \qquad \gamma_{\mathrm{CFL}_{2\pi}} = 2\pi\left[1 - \frac{2(g-\Delta)m}{\sqrt{[2(g-\Delta)m]^2 + K_F^4}}\right], \\ k_{\mathrm{CFL}_0} &= 0, \qquad \gamma_{\mathrm{CFL}_0} = -2\pi\frac{mK_F^2}{8g\Delta^2} + \mathcal{O}\left(\frac{K_F^4}{\Delta^4}, \frac{m^2}{g^2}\right), \end{aligned} \tag{16}$$

where K_F is the Fermi wave vector. As Fig. 4(b) illustrates, when $m \to \infty$ we asymptotically recover $\tilde{\sigma}_{xy} = 1$ starting from $\mathrm{CFL}_{2\pi}$ or CFL_0, consistent with the HLR result.

Distinctions between bosonic CFLs.—A quantitative (but nonuniversal) difference between CFL_0 and $\mathrm{CFL}_{2\pi}$ can be found in the crossover of $\tilde{\sigma}_{xy}$ from zero to unity upon breaking particle-hole symmetry; cf. Eq. (16) and Fig. 4(b). While $\tilde{\sigma}_{xy}$ is not directly observable, Ref. [8] suggested that it may be determined from detailed Hall-effect measurements; Ref. [43] suggested the Nernst effect as a more sensitive $\tilde{\sigma}_{xy}$ probe.

Distinguishing between $\mathrm{CFL}_{2\pi}$ and CFL_0 in the presence of both $\mathcal{I}$ and $\mathcal{C}$ is more subtle; operators constructed from composite fermions near the Fermi surface do not distinguish between the two. Still, the two clearly differ in the limit of low composite-fermion density $K_F \ll \Delta, g$ in the same way that bilayer graphene is distinct from 2D electron gases with parabolic dispersion [44] (see also Supplemental Material [29]). For example, Eq. (16) implies that for $\mathrm{CFL}_{2\pi}$ the susceptibility $\chi \equiv (\partial\tilde{\sigma}_{xy})/(\partial m)|_{m\to 0} \sim 1/K_F^2$ diverges as $K_F \to 0$, whereas for CFL_0 $\chi \sim K_F^2$ and thus vanishes.

Alternatively, consider the 3D SPT surface, which permits reversing the magnetic field while preserving all symmetries. In $\mathrm{CFL}_{2\pi}$ this amounts to smoothly sweeping the composite-fermion chemical potential μ_{CF} between the quadratically touching bands. The SPT surface remains in gapless CFL throughout, up to marginal effects precisely at $B = 0$. In contrast, sweeping μ_{CF} between positive- and negative-energy bands in CFL_0 yields a composite-fermion band insulator at an intermediate stage, which corresponds to a physical superfluid [25,26].

Gapped phases.—It is well known that Cooper-pairing composite fermions generates a quantum-Hall insulator of the microscopic particles. As with the HLR theory, it is natural in $\mathrm{CFL}_{2\pi}$ or CFL_0 to consider chiral, odd-angular-momentum pairing between composite fermions—which permits a full gap for spinless fermions. Such states always break $\mathcal{C}$ [31]. An alternative gapped phase arose in the study of time-reversal-symmetric surfaces of 3D bosonic SPTs in Ref. [32]. In our network model, this phase arises from the edge-boson interaction

$$\mathcal{L}_{2\sigma^x} = \sum_{\alpha,y} u_\alpha \cos\left(\phi_{y-1,\alpha} - 2\phi_{y,\alpha} + \phi_{y+1,\alpha}\right), \tag{17}$$

where $u_+ \neq u_-$ results in a $\mathcal{C}$-symmetric—but not $\mathcal{I}$-symmetric—topological order with $K = 2\sigma^x$ [45]. ($\mathcal{I}$ interchanges u_+ and u_-, with the gap closing when $u_+ = u_-$.)

A symmetric gapped state is nevertheless readily constructed as a composite-fermion superconductor driven by $\mathcal{L}_{\mathrm{Pair}} \sim \Psi_4^\dagger \sigma^y \tau^x \Psi_4^\dagger + \mathrm{H.c.}$ We expect that this state corresponds to a "larger" topological order that can be reduced to $K = 2\sigma^x$ by condensing an $\mathcal{I}$-odd boson. Edge-boson interactions that generate such a state may be obtained by following Refs. [18,45,46], but that is not our focus. We simply note that, in $\mathrm{CFL}_{2\pi}$ and CFL_0 with a single Fermi surface, $\mathcal{L}_{2\sigma^x}$ and $\mathcal{L}_{\mathrm{Pair}}$ are both absent in the projected Hilbert space. Accessing either $\mathcal{C}$-symmetric gapped state

requires a finite coupling strength. Conversely, any gapped state emerging from a weak-coupling instability of $\mathrm{CFL}_{2\pi}$ or CFL_0 necessarily breaks $\mathcal{C}$.

Conclusions.—We constructed two PH-symmetric metallic states, dubbed $\mathrm{CFL}_{2\pi}$ and CFL_0, for bosons at $\nu = 1$. These phases are distinct, provided PH and inversion symmetries are present. In either case, $2K_F$ oscillations in the physical boson density are absent but appear when PH symmetry is broken. Furthermore, once PH symmetry is (weakly) broken, the crossover between these states and the conventional HLR theory may be observed in transport measurements. We also elucidated the relationship between PH-symmetric CFLs and gapped quantum Hall states, such as the bosonic Moore-Read state which breaks PH symmetry and the $K = 2\sigma^x$ state which does not.

A recent study by Wang and Senthil [31] considers bosons at $\nu = 1$ in the LLL with PH symmetry and proposes a CFL with Berry phase -2π. We believe that the states introduced here are closely related; we emphasize, however, that inversion symmetry is crucial in our setup to define a Berry phase of 2π.

We gratefully acknowledge T. Senthil, C. Kane, M. Metlitski, and D. T. Son for valuable discussions. This work was supported by the National Science Foundation (NSF) through Grants No. DMR-1341822 (J. A.) and No. DMR-1206096 (O. I. M.); the Caltech Institute for Quantum Information and Matter, a NSF Physics Frontiers Center with support of the Gordon and Betty Moore Foundation; and the Walter Burke Institute for Theoretical Physics at Caltech.

[1] B. I. Halperin, P. A. Lee, and N. Read, Phys. Rev. B **47**, 7312 (1993).
[2] R. L. Willett, M. A. Paalanen, R. R. Ruel, K. W. West, L. N. Pfeiffer, and D. J. Bishop, Phys. Rev. Lett. **65**, 112 (1990).
[3] W. Kang, H. L. Stormer, L. N. Pfeiffer, K. W. Baldwin, and K. W. West, Phys. Rev. Lett. **71**, 3850 (1993).
[4] V. J. Goldman, B. Su, and J. K. Jain, Phys. Rev. Lett. **72**, 2065 (1994).
[5] S. D. Sarma and A. Pinczuk, *Perspectives in Quantum Hall Effects: Novel Quantum Liquids in Low-Dimensional Semiconductor Structures* (Wiley, Chichester, 1996).
[6] R. L. Willett, Adv. Phys. **46**, 447 (1997).
[7] J. K. Jain, *Composite Fermions* (Cambridge University Press, Cambridge, 2007).
[8] D. T. Son, Phys. Rev. X **5**, 031027 (2015).
[9] N. Read, Semicond. Sci. Technol. **9**, 1859 (1994).
[10] R. Shankar and G. Murthy, Phys. Rev. Lett. **79**, 4437 (1997).
[11] D.-H. Lee, Phys. Rev. Lett. **80**, 4745 (1998).
[12] V. Pasquier and F. Haldane, Nucl. Phys. **B516**, 719 (1998).
[13] M. A. Metlitski and A. Vishwanath, Phys. Rev. B **93**, 245151 (2016).
[14] C. Wang and T. Senthil, Phys. Rev. B **93**, 085110 (2016).
[15] S. D. Geraedts, M. P. Zaletel, R. S. K. Mong, M. A. Metlitski, A. Vishwanath, and O. I. Motrunich, Science **352**, 197 (2016).
[16] G. Murthy and R. Shankar, Phys. Rev. B **93**, 085405 (2016).
[17] S. Kachru, M. Mulligan, G. Torroba, and H. Wang, Phys. Rev. B **92**, 235105 (2015).
[18] D. F. Mross, J. Alicea, and O. I. Motrunich, Phys. Rev. Lett. **117**, 016802 (2016).
[19] M. Mulligan, S. Raghu, and M. P. A. Fisher, Phys. Rev. B **94**, 075101 (2016).
[20] A. C. Balram and J. K. Jain, Phys. Rev. B **93**, 235152 (2016).
[21] Technically, the model studied here requires disorder or a superlattice to describe a plateau transition.
[22] T. Senthil and M. Levin, Phys. Rev. Lett. **110**, 046801 (2013).
[23] Y.-M. Lu and A. Vishwanath, Phys. Rev. B **86**, 125119 (2012).
[24] S. D. Geraedts and O. I. Motrunich, Ann. Phys. (Amsterdam) **334**, 288 (2013).
[25] T. Grover and A. Vishwanath, Phys. Rev. B **87**, 045129 (2013).
[26] Y.-M. Lu and D.-H. Lee, Phys. Rev. B **89**, 195143 (2014).
[27] A. Vishwanath and T. Senthil, Phys. Rev. X **3**, 011016 (2013).
[28] A. H. Castro Neto, F. Guinea, N. M. R. Peres, K. S. Novoselov, and A. K. Geim, Rev. Mod. Phys. **81**, 109 (2009).
[29] See Supplemental Material at http://link.aps.org/supplemental/10.1103/PhysRevLett.117.136802 for details of a coupled-wire description of bosonic $\nu = 2$ IQH states; composite-fermion band structure; Berry phases; projection onto quadratically touching bands; and citation of Ref. [30].
[30] J. C. Y. Teo and C. L. Kane, Phys. Rev. B **89**, 085101 (2014).
[31] C. Wang and T. Senthil, arXiv:1604.06807.
[32] A. Vishwanath and T. Senthil, Phys. Rev. X **3**, 011016 (2013).
[33] One can alternatively view PH as a time-reversal symmetry, as done earlier in Ref. [32], where this SPT was labeled $U(1) \times Z_2^{\mathrm{T}}$.
[34] C. Wang and T. Senthil, Phys. Rev. X **5**, 041031 (2015).
[35] T. Senthil and M. P. A. Fisher, Phys. Rev. B **74**, 064405 (2006).
[36] C. Wang and T. Senthil, Phys. Rev. X **6**, 011034 (2016).
[37] C. Xu and Y.-Z. You, Phys. Rev. B **92**, 220416 (2015).
[38] O. Aharony, J. High Energy Phys. 02 (2016) 093.
[39] A. Karch and D. Tong, arXiv:1606.01893 [Phys. Rev. X (to be published)].
[40] N. Seiberg, T. Senthil, C. Wang, and E. Witten, arXiv:1606.01989.
[41] We performed a change of basis relative to Ref. [18] that results in $\tau^z\sigma^z \to \tau^x\sigma^x$.
[42] An additional allowed term $g'(\tau^x\sigma^y - \tau^y\sigma^x)$ can be rotated onto g; see Supplemental Material [29].
[43] A. C. Potter, M. Serbyn, and A. Vishwanath, Phys. Rev. X **6**, 031026 (2016).
[44] K. S. Novoselov, E. McCann, S. V. Morozov, V. I. Fal'ko, M. I. Katsnelson, U. Zeitler, D. Jiang, F. Schedin, and A. K. Geim, Nat. Phys. **2**, 177 (2006).
[45] D. F. Mross, A. Essin, and J. Alicea, Phys. Rev. X **5**, 011011 (2015).
[46] D. F. Mross, A. Essin, J. Alicea, and A. Stern, Phys. Rev. Lett. **116**, 036803 (2016).